

Influence of solar activity changes on European rainfall

Ludger Laurenz^a, Horst-Joachim Ludecke^b, Sebastian Luning^{c,1}

a Independent Researcher, Münster, Germany

b University of Applied Sciences HTW, Saarbrücken, Germany

c Institute for Hydrography, Geoecology and Climate Sciences, Hauptstraße 47, 6315, Ägeri, Switzerland

Non layout-version of Laurenz et al., 2019, Journal of Atmospheric and Solar-Terrestrial Physics 185 (2019) 29-42

Abstract

European hydroclimate shows a high degree of variability on every time scale. The variability is controlled by natural processes such as Atlantic ocean cycles, changes in solar activity, volcanic eruptions and anthropogenic factors. This contribution concentrates on the solar influence on European precipitation, a relationship which has been documented by a large body of published case studies. Here we are concentrating on the period 1901–2015 for which we compare sunspot data with monthly precipitation series of 39 European countries by calculating Pearson correlation coefficients for a multi-year cross-correlation window. The coefficients have been mapped out across Europe with the aim to identify areas in which solar activity may have influenced precipitation. Results show that February precipitation in Central and Western Europe yields the strongest solar response with coefficients reaching up to +0.61. Rainfall in June–July is equally co-driven by solar activity changes, whereby the solar-influenced zone of rainfall shifts from the British Isles towards Eastern Europe during the course of summer. Other months with noteworthy solar responses are April, May and December. On a decadal scale, the correlation between precipitation and solar activity in central Europe appears to be mostly positive, both statistically and by visual curve comparison. Yet, best positive correlations coefficients of February, June, July and December are typically reached when the solar signal lags rainfall by 1.5–2 years. Taking into account cause and effect, it is suspected that increases in Central European rainfall are actually triggered by the solar minimum some 3–4 years before the rainfall month, rather than the lagging solar maximum. Similar lags of a few years occur between solar activity and the solar-synchronized North Atlantic Oscillation (NAO) due to memory effects in the Atlantic. The literature review demonstrates that most multidecadal studies from Central Europe encountered a negative correlation between solar activity and rainfall, probably because short time lags of a few years are negligible on timescales beyond the 11 year solar Schwabe cycle. Flood frequency typically increases during times of low solar activity associated with NAO-conditions and more frequent blocking.

1. Introduction

European hydroclimate shows a high degree of variability on diverse time scales, reaching from daily to millennial (e.g. [Linderholm et al., 2018](#); [Magny, 2004](#); [Markonis et al., 2018](#); [Zveryaev and Allan, 2010](#)). This variability in rainfall, floods and droughts is thought to be controlled by natural processes such as Atlantic ocean cycles (e.g. [Hurrell and van Loon, 1997](#); [Trigo et al., 2004](#)), changes in solar activity (e.g. [Czymzik et al., 2016b](#)) and volcanic eruptions (e.g. [Rao et al., 2017](#)), as well as by anthropogenic factors (e.g. [Maraun, 2013](#)). A robust understanding of natural precipitation drivers is necessary in order to reliably distinguish their effects from anthropogenic influences. This is particularly important for climate models which need to take all possible forcing factors qualitatively

¹ Corresponding author. *E-mail addresses:* moluedecke@t-online.de (H.-J. Ludecke), luning@ifhgw.org (S. Luning).

and quantitatively into account in order to continuously improve their hindcast and forecast performances ([Bothe et al., 2018](#); [DeAngelis et al., 2015](#); [Hoerling et al., 2009](#)). In this contribution we are concentrating on the potential influence of solar activity changes on European rainfall. In the first part, we are reviewing the existing literature on the subject, focussing on regional trends, time lags and methodologies. In the second part of this paper we are comparing regional European rainfall series of the past 115 years with solar activity indices by means of statistical analyses. The objective is to test for possible correlations on yearly, seasonal and monthly resolutions.

2. Solar influence on European rainfall

Various papers have suggested a solar influence on European rainfall. Here we are reviewing this evidence, regionally grouped for western, northern, eastern and southern Europe. The studies use modern rainfall and river discharge data, as well as palaeoclimate proxies for wetlands humidity and river floods. Time scales reach from the solar Schwabe cycle (11 years) to the solar Hallstatt cycle (2300 years).

2.1. Western Europe

The solar Schwabe cycle appears to play a major role for summer flooding in the European Alps. The flood frequency of River Ammer in the Bavarian Alpine Foreland typically increases during intervals of reduced solar activity. Significant correlations have been identified between late spring/summer discharge data of the last 90 years and solar activity ([Czymzik et al., 2016b](#)). Interestingly, the solar influence on hydroclimate appears somewhat delayed, as the flood record lags the solar signal by 2–3 years. The 11 years solar cycle was also found in a cross-spectral analysis of summer floods in Switzerland of the past 200 years ([Peña et al., 2015](#)). As in River Ammer, flooding was more frequent during solar activity minima. Nonlinear spectral analysis of Holocene varves in a Westeifel crater lake of Holzmaar (western Germany) also yielded a Schwabe cycle periodicity ([Negendank et al., 1997](#); [Vos et al., 1997, 2004](#)), even though it is unclear whether hydroclimate or temperature changes are the main climatic driver. Solar-driven changes in discharge of river Rhine at Basel were suggested by [Franke and Bechteler \(1969\)](#) involving alternating phase shifts and 2–3 years time lags. [Vines \(1985\)](#) proposed various periodicities for European rainfall, including Schwabe and Hale (22 years) cyclicity.

Solar influence on European hydroclimate has been also reported on a centennial to multi-centennial scale comprising of the Gleissberg (80–100 years) and Suess – de Vries (210 years) solar cycles. In the northern and central Alps, multidecadal summer flood-prone periods typically occurred when solar activity was reduced. Varve studies in the Bavarian Lake Ammersee for the past 450 years document an increase in spring and summer floods during the Sporer, Maunder, and Dalton solar minima of the Little Ice Age (LIA) ([Czymzik et al., 2010](#)). Holocene summer flood frequency in the Central Alps is pulsed by Gleissberg and Suess – de Vries solar periodicities, as evidenced in lake sedimentary cores in Switzerland and northern Italy ([Rabadan and Schulte, 2014](#); [Schulte et al., 2015](#); [Wirth et al., 2013b](#)). In an analysis of historical floods in Switzerland of the past 200 years, Peña et al. (2015) identified a clear Gleissberg cyclicity. All Swiss studies agree that summer flood frequency was higher during solar activity minima. Nevertheless, regional differences between the Northern and Southern Alps have been observed and need to be taken into account ([Pena et al., 2015](#); [Wirth et al., 2013b](#)). Gleissberg and Suess-de Vries solar periodicities have been documented in Holocene

hydroclimate reconstructions studying lake and wetlands cores in Germany ([Czymzik et al., 2016a](#); [Negendank et al., 1997](#); [Vos et al., 1997](#)), the Netherlands ([Blaauw et al., 2004](#)), UK ([Macklin et al., 2005](#); [Mauquoy et al., 2002, 2004](#); [Swindles et al., 2007b, 2012](#)) and Ireland ([Blackford and Chambers, 1995](#); [Stolze et al., 2013](#)). In most cases, wet periods fall into low solar activity phases. In contrast, [Nurtaev \(2015\)](#) suggested a positive correlation between sunspots and river Rhine discharge for the past 100 years.

Solar activity appears to also play a role for rainfall in Western Europe on even longer time scales, namely through the solar cycles of 500 years and the millennial-scale 1000 years (Eddy) and 2300 years (Hallstatt) periodicities. These cycles were documented for flood histories in southern Germany ([Czymzik et al., 2013](#)) and Switzerland ([Schulte et al., 2009](#); [Wirth et al., 2013b](#)), lake levels in Switzerland and France ([Magny, 1993, 2004](#)), and wetlands humidity changes in the UK and Denmark ([Mauquoy et al., 2008](#); [Swindles et al., 2007b, 2010, 2012](#)). Time lags for full hydroclimate response of up to 50 years have been reported by [Mauquoy et al. \(2008\)](#). More humid conditions typically prevailed during phases of low solar activity. A particularly wet and cold episode occurred in Western Europe during the so-called 2.8 kyr BP event, the Homeric Minimum, a phase of low solar activity that took place around 2800 years ago and persisted for more than 150 years (e.g. [Bond et al., 2001](#)). The associated dramatic increase in humidity has been documented in Germany ([Martin-Puertas et al., 2012](#)), the Netherlands ([Kilian et al., 1995](#); [van Geel et al., 2014](#); [van Geel and Mauquoy, 2010](#); [Van Geel et al., 1997](#)) and the UK ([Swindles et al., 2007a](#)).

Solar activity also affects wind regimes in Central Europe. [Schwander et al. \(2017\)](#) analysed weather types for the past 250 years and found fewer days with westerly and west south-westerly flow over Central Europe under low solar activity, hereby northerly and easterly flow types increased. The blocking frequency between Iceland and Scandinavia increases during solar minima and Central European temperatures cool. Notably, model simulations are still not able to reproduce this imprint of the 11-year solar cycle on the tropospheric weather of the region ([Schwander et al., 2017](#)).

2.2. Northern Europe

The phase relationship between solar activity and precipitation appears to be regionally differentiated in northern Europe. Studies from southern and central Sweden document a marked increase in precipitation and floods during the 2.8 kyr BP grand solar minimum ([Labuhn et al., 2018](#); [Mellstrom et al., 2015](#)). In northern Sweden, however, summer rainfall increases in high solar activity phases, as documented by [Kokfelt and Muscheler \(2013\)](#) for the past 1000 years in a lake sedimentary core. Rainfall was reduced during the Wolf, Sporer and Maunder solar minima. [Kokfelt and Muscheler \(2013\)](#) also compared the sunspot cycle with a long instrumental series of summer precipitation at the Abisko Scientific Research Station in northern Sweden for the past 100 years. Whilst the first half of the series 1920–1960 lacked a robust link, the second half 1960–2000 yielded statistically significant correlations. As in the multi-centennial reconstruction, the amount of summer precipitation increased during periods with higher solar activity. In Latvia, [Hajian and Movahed \(2010\)](#) presented a comparison of sunspots and discharge of the river Daugava. The authors identified a cyclical element in the river flow that showed some similarities with solar activity although with a periodicity closer to the solar Hale cycle (22 years).

2.3. Eastern Europe

A shift towards a wetter and colder climate in association with the 2.8 kyr solar minimum was described by [Speranza et al. \(2003\)](#) for the Czech Republic. Discharge of Elbe River at Děčín in the northern Czech Republic shows alternating correlations with sunspots during the period 1850–1960 (Franke and Bechteler, 1969). [Nurtaev \(2015\)](#) compared Danube River discharge with solar activity for the past 100 years and found an inverse correlation, with higher flow rates during weak solar phases. [Ducic et al. \(2007\)](#) tested various combinations of solar and lower Danube discharge parameters in the Romanian-Serbian segment and found the best correlations between flow index and latitude of sunspots. [Mares et al. \(2016\)](#) studied the same lower Danube discharge data and found maximum spring and summer flow rates about 2–3 years after solar Schwabe minima. The geomagnetic index aa as solar proxy produced the best results. [Dobrica et al. \(2017\)](#) analysed the power spectrum of the lower Danube discharge and identified periods that are linked to the solar Schwabe and Hale cycles and their multiples. [Lamy et al. \(2006\)](#) studied the Holocene discharge history of Sakarya River which represents Anatolia's longest river. Maximum discharge was found to be associated with periods of reduced solar activity, similar as in the case of the Danube.

2.4. Southern Europe

Variability in Italian precipitation and floods is controlled by the North Atlantic Oscillation (NAO) and solar activity ([Brunetti et al., 2000](#); [Wirth et al., 2013a](#)). [Zanchettin et al. \(2008\)](#) analysed Po River discharge and northern Italian regional precipitation data and found that wet and dry periods alternate in accordance with polarized sunspot cycles, i.e. solar Hale cycles. Solar forcing is assumed to take place via the solar-forced NAO. Positive (negative) NAO anomalies are associated with comparatively lower (higher) Po River discharges ([Zanchettin et al., 2008](#)). The strength of solar activity is thought to modulate the connection between the NAO and Po River discharges. [Landscheidt \(2000\)](#) in response to [Tomasino and Valle \(2000\)](#) pointed to phase shifts in the solar influence on Po River discharge over the past 100 years. Based on the observed patterns, [Tomasino et al. \(2004\)](#) suggested that Po River discharge may be predictable based on solar activity periodicities. Periodicities associated with the Schwabe solar cycle and the NAO have also been reported from sedimentary cores in the Gulf of Taranto located at the distal end of the Po-river discharge plume ([Chen et al., 2011](#); [Cini Castagnoli et al., 2002](#)). Notably, Summer precipitation trends have been anti-correlated in northern and southern Italy during the past 150 years ([Brunetti et al., 2000](#)).

Climate reconstructions for the past 2000 years in Lake Ledro in the Italian Southern Alps found an increase in flooding during phases of low solar activity, namely in the Dalton, Sporer, Maunder, and Wolf Minima ([Vanniere et al., 2013](#); [Wirth et al., 2013a](#)). The northern Italian rivers Tiber, Adige and Po show a maximum in flooding frequency during the Sporer Minimum ([Camuffo and Enzi, 1995](#); [Glaser et al., 2010](#)). Tiber and Adige experienced another flooding maximum at the onset of the Maunder Minimum ([Glaser et al., 2010](#)). In Iberia, the relationship between floods and solar activity is opposite to that in Italy. Reconstructions from Spain for the last 1000 years show a decrease of flood frequency during solar minima in late summer and autumn ([Barrera-Escoda and Llasat, 2015](#); [Corella et al., 2014](#); [Glaser et al., 2010](#); [Moreno et al., 2008](#); [Vaquero, 2004](#)). [Smith et al. \(2016\)](#) documented millennial-scale hydroclimatic cycles from a northern Spanish cave which appear to be linked to a cyclicity that [Bond et al. \(2001\)](#) associated with solar activity changes.

2.5. Complexity of the solar signal

The literature review shows that the solar influence on European precipitation follows certain patterns, yet in a complex way. The correlation coefficients between hydroclimate and solar activity keep changing on regional and temporal scales ([Le Mouel et al., 2009](#)). Regional differences occur and reflect the dominance of different atmospheric regimes resulting in opposite solar effects. Typical time lags of a few years point to delayed climatic response due to the inertia of the oceans which play an important additional role for variability in European rainfall. Once fully understood, the lags may offer seasonal rain forecasts. Solar effects on precipitation have been observed on time scales ranging from Schwabe (11 years) to Hallstatt (2300 years) cycles and also differ for separate seasons and months. The coupling between solar activity and rainfall is variable and includes periods with stronger and other periods with weaker correlation.

3. Material and methods

3.1. Data

In order to test for possible correlations between rainfall and solar activity, monthly precipitation data for 39 European countries covering the period 1901–2015 was downloaded from the Climate Change Knowledge Portal which is operated by the World Bank Group (<http://sdwebx.worldbank.org/climateportal/>). This gridded historical dataset is derived from observational data and has been produced by the Climatic Research Unit (CRU) of the University of East Anglia, reformatted by the International Water Management Institute. The CRU dataset shows reasonably consistent interannual variability compared to other gauge-based precipitation datasets, namely those from the Global Precipitation Climatology Centre (GPCC) and the University of Delaware (UDEL), even though with deviations in magnitudes of up to about 100mm ([Sun et al., 2018](#)). In order to extend the rainfall record into the 19th and 18th centuries, three additional long term data series were included in the analysis. The Stockholm data set reaches back to 1786 and was sourced from the Swedish Meteorological and Hydrological Institute (<http://opendata-download-metobs.smhi.se/explore/>). A historical precipitation series from Paris covers the period 1804–1919, kindly provided by Météo-France. This series contained minor (< 2%) data gaps which were filled by interpolation. The Edinburgh series covers the period 1785–2002 and was sourced from the UK Met Office National Meteorological Archive. The sunspot data is based on Sunspot Number Version 2.0 from the Royal Observatory of Belgium in Brussels, Sunspot Index and Long-term Solar Observations (<http://www.sidc.be/silso/datafiles>), ([Clette et al., 2015](#)).

3.2. Statistical processing

Both the monthly precipitation and sunspot data were smoothed using a Savitzky-Golay Filter (SGF). The SGF is a method of filtering the data for increasing the signal-to-noise ratio. The fundamental method is mathematical convolution ([Riley et al., 2006](#)) by fitting successive sub sets of close-by data points with a polynomial by the linear least squares method ([Luo et al., 2005](#); [Savitzky and Golay, 1964](#)). In most cases, SGF gives better results than smoothing by a simple moving average (SMA). Supplement Figs. S20–21 visualize the SGF applied on a graph of this paper by comparing it with the unfiltered data and with a simple moving average of width 3 (SMA). The SGF used here, generally, has a frame size of 11 and a polynomial order of 5 for both precipitation and sunspots.

Monthly precipitation per country and sunspots were compared by calculating Pearson correlation coefficients. In order to allow for lead/lag relationships, a cross correlation window of -120 to $+24$ months was chosen. While the rainfall was kept stable, the solar signal preceding the rainfall by up to 120 months (negative solar lag, i.e. lead) or postdating the rainfall by up to 24 months (positive solar lag) was shifted onto the rain series. The coefficient of the most positive correlation in this window was recorded, together with the solar lag in full months (Table 1 and S1; see illustrated time series for all countries in Supplement Figs. S1 and S2). In a parallel exercise, the most negative correlation coefficients and their respective lag were recorded for a slightly shortened cross correlation window of -80 and $+24$ months (Tables S2 and S3). Window shortening was empirically found necessary in order to obtain more consistent results. Selected rainfall series were studied by means of wavelet analysis ([Grinsted et al., 2004](#)).

In order to ascertain the statistical confidence of the Pearson correlation r between precipitation and Sunspot time series over 1901 to 2015, we assumed the null hypothesis that r is caused by chance. We evaluated this assumption by Monte Carlo simulation (MC) ([Mazhrakov et al., 2018](#)) based on surrogate records of the same Hurst exponent H as the European precipitation time series. We evaluated H by the detrended fluctuation analysis of the European country precipitations ([Kantelhardt et al., 2001](#)) with the result of $H \approx 0.6$, which means only weak autocorrelation (white noise as $H=0.5$). $H \approx 0.6$ was also found by J. W. Kantelhardt for worldwide precipitation time series ([Kantelhardt, 2004](#)). In the MC simulation 10,000 surrogates replaced the real monthly precipitation time series. Both for the surrogates and the sunspot number series the same Savitzky-Golay filter of frame size 11 and polynomial order 5 was used. The surrogates were generated by a standard method ([Turcotte, 1997](#)). As a result, we found the following probabilities p for the null hypothesis: For values of $|r| > 0.45$ $p < 0.001$, for $|r| > 0.35$ $p < 0.01$, and for $|r| > 0.25$ $p < 0.05$.

4. Results

The correlation between monthly precipitation and sunspots of the period 1901–2015 shows significant regional and seasonal variability (Tables 1 and S2). Pearson coefficients vary from 0.61 (Liechtenstein, February) to -0.53 (Estonia, February), representing correlations ranging from moderate positive to moderate negative. The best positive correlations occur during February when 7 out of the 39 countries achieve coefficients of 0.50 or better (Tables 1 and 2). February also shows the best negative correlations, although with slightly weaker strength than the positive correlations (Tables 2 and S2). Significant parts of Europe yield moderate to low positive correlations during the months of April, June, July and December (Tables 1 and 2). The month of May differs because the best coefficients are negative correlations, with 9 countries showing r values of -0.35 and better (Tables 2 and S2). The remaining six months (January, March, August, September, October, November) show weaker coefficients, suggesting somewhat reduced solar influence on precipitation during these times. The results of all months were mapped out in order to see if regional patterns can be identified. The months with the best results are illustrated here in the main paper (Figs. 3, 4, 6–8), and the remaining months are contained in the Supplement (Figs. S3–S9).

4.1. January

January precipitation variability is only weakly correlated with solar activity. Regions with low correlation strengths are scattered across Europe, namely eastern Scandinavia, the southern North Sea countries, Spain, Switzerland and parts of the Balkans (Fig. S3).

Table 1

Correlation coefficients of precipitation vs. sunspots, interval 1901–2015, by European country. The values represent the **most positive** results in a cross correlation window of -120 to $+24$ months. Respective solar lags are shown in Table S1. Coefficients ≥ 0.40 are highlighted in bold red, coefficients 0.30 – 0.39 are marked in bold blue. p is the probability that the correlation r is by chance (false alarm probability). For values of $|r| > 0.45$ $p < 0.001$; for $|r| > 0.35$ $p < 0.01$; and for $|r| > 0.25$ $p < 0.05$.

	Jan	Feb	Mar	Apr	May	Jun	Jul	Aug	Sept	Oct	Nov	Dec
Albania	0.08	0.35	0.22	0.34	0.13	0.14	0.14	0.12	0.09	0.10	0.31	0.35
Austria	0.11	0.44	0.40	0.13	0.35	0.40	0.48	0.13	-0.01	0.10	0.19	0.21
Belarus	0.17	0.18	0.30	0.22	0.37	0.20	0.33	0.35	0.23	0.22	0.10	0.33
Belgium	0.33	0.51	0.28	0.41	0.30	0.36	0.23	0.16	0.27	0.05	0.30	0.37
Bosnia and Herz.	0.12	0.23	0.19	0.12	0.15	0.17	0.09	0.12	0.09	0.00	0.17	0.32
Bulgaria	0.14	0.34	0.19	0.29	0.15	0.18	0.20	0.22	0.07	0.00	0.37	0.35
Croatia	0.14	0.11	0.13	0.13	0.16	0.24	0.19	0.17	0.06	0.11	0.13	0.19
Czech Republic	0.07	0.42	0.28	0.12	0.40	0.43	0.38	0.12	0.11	0.16	0.20	0.26
Denmark	0.30	0.42	0.29	0.26	0.19	0.30	0.19	0.28	0.24	0.21	0.29	0.16
Estonia	0.29	0.52	0.29	0.33	0.13	0.11	0.39	0.18	0.38	0.33	0.13	0.09
Faroe Islands	0.04	0.17	0.48	0.37	0.22	0.22	0.15	0.23	0.23	0.19	0.18	0.27
Finland	0.25	0.34	0.38	0.17	0.07	0.10	0.16	0.29	0.30	0.24	0.13	0.15
France	0.21	0.42	0.08	0.17	0.14	0.19	0.12	0.30	0.29	0.29	0.19	0.30
Germany	0.21	0.54	0.39	0.27	0.38	0.46	0.16	0.18	0.20	0.13	0.28	0.37
Greece	0.21	0.30	0.15	0.39	0.09	0.01	0.22	0.11	0.10	0.09	0.26	0.35
Hungary	0.13	0.19	0.14	0.06	0.21	0.42	0.39	0.21	0.05	0.04	0.28	0.29
Iceland	0.15	0.48	0.32	0.28	0.31	0.53	0.26	0.20	0.04	0.38	0.14	0.41
Ireland	0.13	0.33	0.13	0.16	0.20	0.50	0.02	0.23	0.32	0.35	0.21	0.16
Italy	0.13	0.17	0.00	0.25	0.10	0.20	0.30	0.28	0.20	0.20	0.25	0.17
Kosovo	0.18	0.45	0.21	0.37	0.24	0.20	0.16	0.13	0.12	-0.03	0.42	0.46
Latvia	0.23	0.40	0.24	0.31	0.27	0.18	0.31	0.24	0.33	0.31	0.14	0.20
Liechtenstein	0.24	0.61	0.43	0.17	0.25	0.39	0.34	0.27	0.09	0.18	0.22	0.20
Lithuania	0.17	0.31	0.26	0.26	0.34	0.34	0.31	0.18	0.30	0.23	0.17	0.25
Luxembourg	0.31	0.51	0.31	0.37	0.22	0.29	0.19	0.21	0.28	0.05	0.28	0.43
Macedonia	0.17	0.38	0.21	0.48	0.16	0.12	0.15	0.13	0.06	0.05	0.38	0.40
Moldova	0.23	0.34	0.09	0.21	0.26	0.18	0.07	0.32	0.33	0.18	0.35	0.44
Montenegro	0.17	0.36	0.22	0.14	0.20	0.23	0.14	0.17	0.12	0.05	0.21	0.38
Netherlands	0.29	0.43	0.32	0.30	0.29	0.41	0.11	0.15	0.19	0.12	0.27	0.34
Norway	0.09	0.21	0.43	0.26	0.17	0.32	0.31	0.43	0.20	0.33	0.10	0.25
Poland	0.10	0.39	0.30	0.37	0.36	0.44	0.36	0.22	0.13	0.14	0.18	0.31
Portugal	0.17	0.46	0.22	0.28	0.33	0.25	0.11	0.31	0.15	0.07	0.21	0.38
Romania	0.27	0.33	0.13	0.23	0.12	0.12	0.14	0.20	0.13	0.03	0.38	0.43
Serbia	0.29	0.37	0.14	0.23	0.26	0.25	0.09	0.14	0.14	-0.04	0.42	0.48
Slovakia	0.07	0.29	0.10	0.17	0.36	0.45	0.37	0.18	0.03	-0.01	0.20	0.24
Slovenia	0.20	0.13	0.09	0.11	0.21	0.29	0.39	0.18	0.02	0.19	0.24	0.08
Spain	0.30	0.35	0.19	0.35	0.27	0.14	0.29	0.35	0.37	0.29	0.14	0.29
Sweden	0.30	0.52	0.36	0.26	0.17	0.17	0.27	0.27	0.35	0.18	0.29	0.35
Switzerland	0.25	0.57	0.32	0.09	0.26	0.28	0.35	0.34	0.17	0.22	0.32	0.21
United Kingdom	0.32	0.40	0.20	0.22	0.25	0.48	0.16	0.11	0.31	0.24	0.34	0.07

Table 2

Number of European countries (total = 39) with low, low to moderate and moderate coefficients for the correlation between precipitation (specified by month) and sunspots, 1901–2015. + = positive, n = negative. Months with maps in Figs. 3, 4, 6–8 are shaded in grey. Positive correlations refer to Table 1, negative correlations to Table S2.

Coefficient	Strength	Jan	Feb	Mar	Apr	May	Jun	Jul	Aug	Sep	Oct	Nov	Dec
0.50 - 0.65	moderate +	-	7	-	-	-	2	-	-	-	-	-	-
0.35 - 0.49	mod-low +	-	16	7	8	6	11	8	3	3	2	6	15
0.25 - 0.34	low +	12	8	11	13	12	8	9	9	9	5	12	11
-0.50 - -0.65	moderate n	-	1	-	-	-	-	-	1	-	-	-	-
-0.35 - -0.49	mod-low n	1	16	2	5	9	4	8	-	2	-	2	2
-0.25 - -0.34	low n	6	14	4	12	12	13	7	12	11	15	9	13

4.2. February

Of all months, February yields the best correlations between precipitation and solar activity. Germany, Luxemburg, Belgium, Liechtenstein, Switzerland, Estonia and Sweden all show coefficients of 0.51–0.61 suggesting moderate correlation. Visual inspection of the temporal development (Fig. 1, S1, S2) suggests that the 11 year Schwabe solar cycle is well represented in the variability of precipitation. This is particular the case during the period from the mid 1920s to the mid 2000s for which the Pearson correlation values would be even higher.

A wavelet analysis of Germany's February precipitation confirms the presence of a ~ 11 year cycle period from the mid 1920s to the mid 2000s (Fig. 2). The cycle appears to be weaker in the 1-2 decades before and after this period.

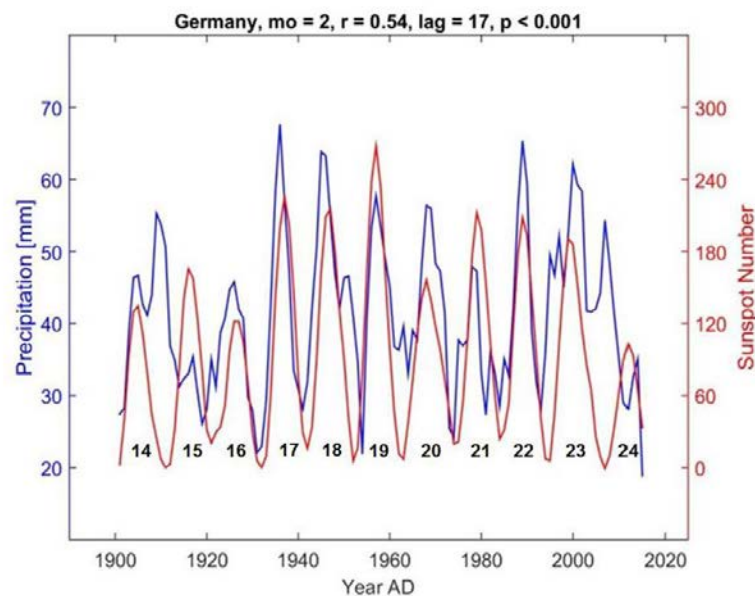


Fig. 1. February precipitation in Germany compared to changes in sunspots. Shown is the optimum positive correlation ($r = 0.54$) with a solar lag of +17 months. Solar cycles are numbered 14–24. The probability that the correlation $r = 0.54$ is by chance is less than 0.1% ($p < 0.001$).

The February correlation sweetspot forms part of a southwest- northeast trending belt stretching from Switzerland to Sweden, characterized by moderate correlation strength (Fig. 3). Slightly weaker but still significant correlations occur in SW and NW Europe as well as in parts of the Balkans. February precipitation in a northeast-trending corridor from the Adriatic Sea to Belarus appears to lack solar influence as Pearson coefficients are statistically insignificant (Fig. 3). Notably, the lag of the optimum correlations changes across Europe. Optimum lag values are +20 months in central Western Europe, -105 months in Sweden and Estonia, and -65 months on the Balkans (Fig. 3), illustrating systematic phase shifts across the continent.

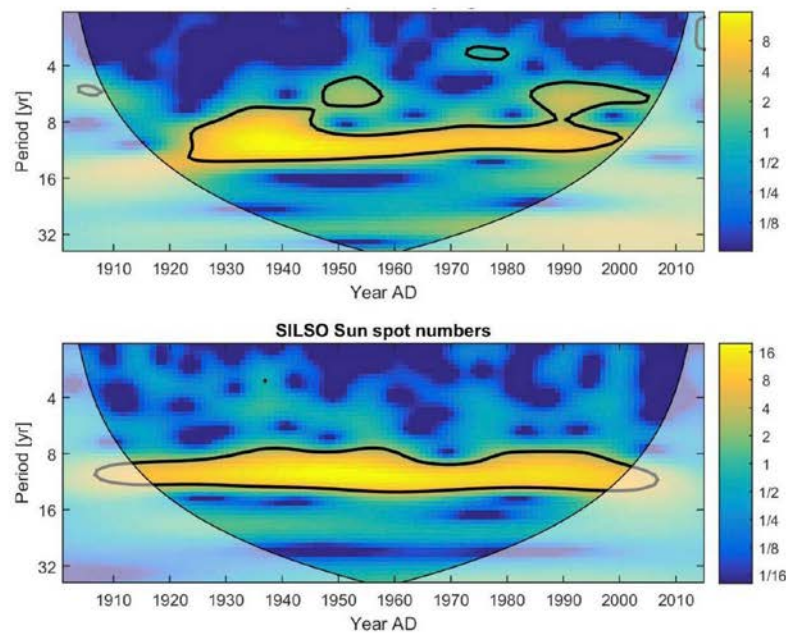


Fig. 2. Wavelet analysis of 1901–2015 February rainfall in Germany (upper chart) and sunspots (lower chart) ($r = 0.54$, solar lag +17 months). Colour legend quantifies wavelet-power. The cone of influence in the wavelet graphs is indicated by a black contour and designates the 5% significance level against red noise.

4.3. March

March precipitation shows a significant solar response in a belt reaching from Austria to Scandinavia where a low to moderate correlation strength with r values of 0.36–0.43 is achieved (Fig. S4). Southern Europe, France and the British Isles lack any indication for solar influence on rainfall. The best coefficients are reached at solar lags of -100 to -110.

4.4. April

During the month of April, low to moderate correlations are developed in parts of Central Europe, SW Europe and Greece (Fig. S5). Low correlations are identified in a N-S corridor stretching from Italy to Scandinavia. About half of Europe lacks evidence for solar influence on April rain, which includes for example the British Isles, France, Finland and central Eastern Europe.

4.5. May

The month of May differs from most other months because the best correlations are characterized by negative coefficients. The best coefficients are reached in a belt from the Czech Republic to Belarus with r values of up to -0.48 (Fig. 4). Significant correlations also exist in neighbouring countries, although slightly weaker. The lag of the best correlations is +15 months, indicating a

general anticorrelation of May rain solar activity in this region, which is also confirmed by visual inspection of the development of the Belarus times series (no lag version, Fig. 5).

4.6. June

The best June correlations occur in NW Europe with r values of 0.50 and better in Ireland and Iceland (Fig. 6). Moderate to low Pearson coefficients are also recorded in a belt reaching from the UK westwards into central Eastern Europe, with a typical solar lag of about -90 months, i.e. the sun leading rainfall by 7.5 years for a positive correlation. Rainfall in southern Europe and eastern Scandinavia appears to generally lack solar influence in June.

4.7. July

The zone of solar-influenced rainfall mapped for June gradually weakens during the course of summer. In July, only the eastern European sector shows moderate to low coefficients while the western sector loses its solar influence altogether (Fig. 7). **4.8. August to October** During the months of August to October, correlations of low and occasionally low to moderate strengths occur in Scandinavia and the Baltic states as well as in SW Europe and France (Figs. S6–S8). The majority of Central and Eastern Europe lack any solar influence. Lags differ between the regions. **4.9. November and December** Compared to previous months, the regional correlation patterns fully change during November. The best correlations are now achieved in the eastern Balkans and western Black Sea regions with r values ≥ 0.35 (Fig. S9). In subsequent December, solar influence further strengthens and regionally expands across many parts of Europe. Besides the Balkans, coefficients of moderate to low strengths also occur in Iceland, Sweden, Germany, Benelux and Portugal (Fig. 8).

4.10. Historical precipitation series

Analysis of the gridded historical CRU dataset covers the past 115 years and shows that solar influence on European rainfall affects certain regions during certain months during certain multidecadal time periods. In the case of February and central Europe, it was shown that the solar signature is only distinctly present from the mid 1920s to the mid 2000s. In order to verify if the solar influence on precipitation also existed during the 19th century, long time series of individual stations or station composites are needed, as European gridded data are not available. Observational precipitation data are available e.g. for Edinburgh, Stockholm and Paris. The historical Edinburgh rainfall series 1785–2002 reaches its best correlation during the month of February with a Pearson r value of +0.35 and a lag of -103 months (Table S4). This matches quite well with the r value of +0.40 calculated for the UK rainfall series 1901–2015 (Table 1). Visual inspection of the historical Edinburgh time series (Fig. S16) as well as the wavelet graphs (Fig. S19) shows that the series contains particular periods in which the correlation breaks down such as in the early and mid 19th Century, apparently partly associated with phase shifts. A better coupling between February rain in Edinburgh and solar activity is observed during the second half of the 19th Century and most of the 20th Century.

Similar discontinuous relationships are seen in the historical precipitation series of Paris and Stockholm (Figs. S17–S19) which demonstrates the complexity of the long term development.

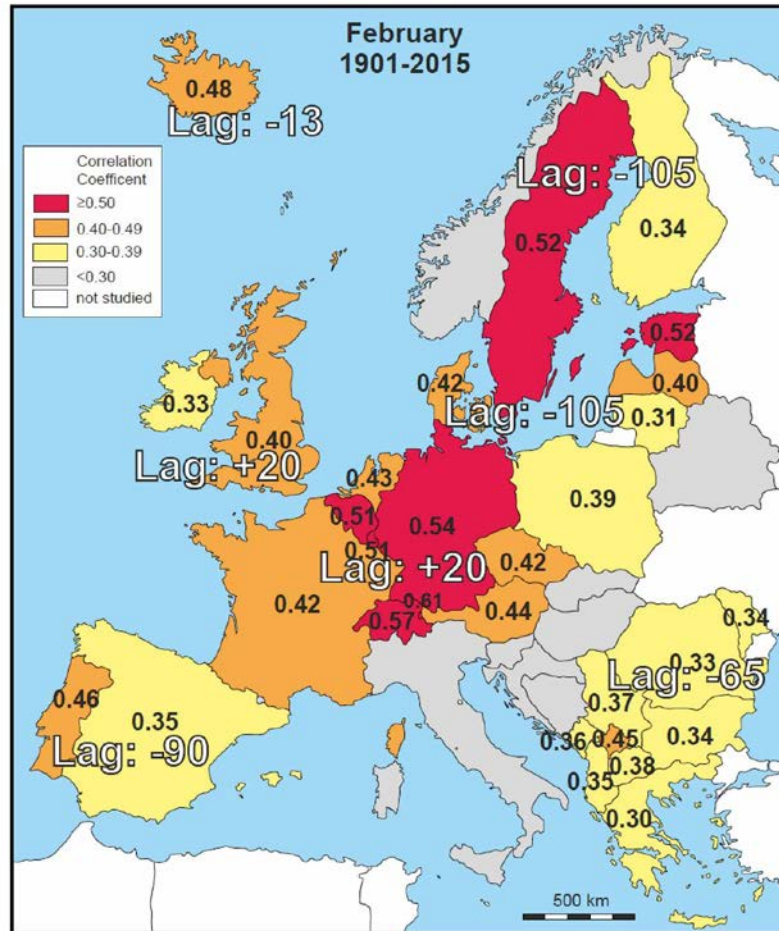


Fig. 3. Map showing the 1901–2015 most positive correlation coefficients for February precipitation and sunspots on a country-by-country basis. Pearson r values from Table 1. All maps: Lags are simplified and generally fall within ± 10 months of the statistically calculated value (Table S1).

4.11. Time lags

In order to identify the best positive and negative correlation coefficients, the sunspot series is progressively shifted against the precipitation series, the latter being kept stable. The cross correlation window encompasses -120 to $+24$ months, i.e. the solar signal precedes the rainfall by up to 120 months (negative solar lag, i.e. lead) or postdates the rainfall by up to 24 months. When plotting the r values against the solar lag for individual monthly country precipitation series, the result is an oscillating curve, with the extreme values represented by the most positive and most negative correlation coefficients. The period of the oscillation corresponds to one ~ 11 year Schwabe solar cycle, whilst the minimum and maximum values are offset by about half a Schwabe cycle. Fig. 9 shows such a plot of r against sun lag for February rain in Germany. The best positive r values are achieved at solar lag times of -110 to -95 and again at $+10$ to $+20$ months. The maxima are about one solar Schwabe cycle apart from each other (11 years = 132 months). The most negative Pearson r values plot in the range of -50 to -35 months, representing a lead time for the solar minimum of 50 to 35 months (=3–4 years) before an increase in rainfall occurs. In the case of February precipitation of Germany, the best positive correlations ($r +0.54$, lag $+17$ months) are numerically better than the best negative correlations ($r -0.35$, lag -37 months) (Tables 1, S1-S3). Notably, in other cases, the reverse is true. February rain in the UK for example has a best positive correlation of $r = +0.40$ (lag $+16$ months), whilst the most negative correlation of $r = -0.47$ (lag -53 months) indicates a better

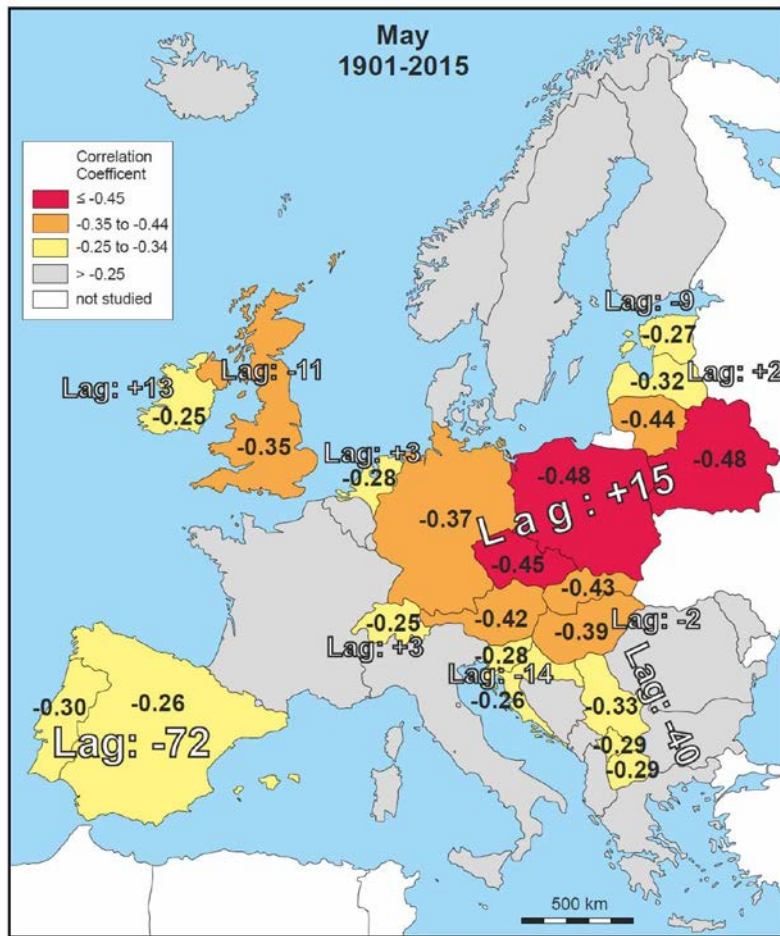


Fig. 4. Map showing the 1901-2015 most negative correlation coefficients for May precipitation and sunspots on a country-by-country basis. Pearson r values from Table S2, lags are from Table S3.

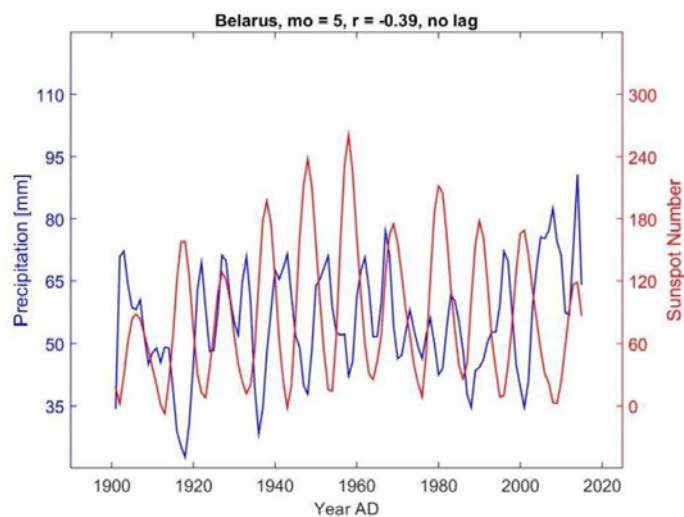


Fig. 5. May precipitation in Belarus compared to changes in sunspots. Shown is the no lag version in which the unshifted monthly May sunspots are plotted. Pearson coefficient is $r = -0.39$. The optimum negative correlation version has a solar lag of +15 months with an r value of -0.48 (see Fig. 4, Tables S2-S3).

correlation strength (Figs. 3 and S11; Tables 1, S1-S3). Another good example is February rain of Estonia in which the best positive correlation ($r = +0.52$, lag -108 months) is very similar to the best negative correlation ($r = -0.53$, lag -41) (Fig. S11, Tables 1, S1-S3). Notably, the best positive correlation in Estonia is not achieved at low positive lags (like in Germany and the UK) but one solar cycle back, with the solar peak leading rainfall by 9 years (Table S1). The solar minimum leads peak February rainfall in Estonia by about three and a half years. The solar lag of the best correlations was schematically mapped in Figs. 3, 4, 6-8, S3-S9. Specific regions consisting of clusters of several countries typically share a similar lag. Systematic shifts in the lag occur across the European continent. Taking the example of February rain, the region stretching from the British Isles across Central Europe to the Baltic Sea area shares a similar lag (Fig. 3). The recorded lag values of -105 and $+20$ months both correspond to the same relationship, i.e. they refer to successive maxima in the 'r against solar lag' plot. The two maxima are offset by one solar Schwabe cycle, whereby the best positive coefficients are mathematically reached in some cases in the high negative and sometimes in the low positive peak, without any greater statistical difference. In contrast, the solar lag for the best positive correlations on the Balkans is around -65 months (Fig. 3), therefore is phase-shifted against the lag in northern Europe by 40 months (~ 3 years) (Fig. S10). Negative r values of February precipitation in Greece ($r = -0.43$, lag -1 month; Tables S2 and S3) document better correlation strength than the positive coefficients ($r = +0.30$, lag -57 months; Tables 1 and S1). This implies a classical inverse relationship between solar activity and February rain in Greece and some other parts of the Balkans.

5. Discussion

The 11 year solar Schwabe "heartbeat" is clearly identifiable in the European precipitation series during certain months, as already suggested by [Vines \(1985\)](#). Regions, strength and solar leads/lags of optimum correlations change across Europe throughout the course of the year, pointing to a complex relationship of solar effects on European precipitation. A better empirical and genetic understanding of these relationships opens up the chance for valuable predictions of precipitation on a regional and seasonal basis.

5.1. February

The best Pearson coefficients of precipitation and sunspots occur in central Western Europe, Sweden and Estonia with r values of ≥ 0.50 . The respective solar lags are $+20$ and -105 months, which are separated by about one solar Schwabe cycle (~ 132 months), therefore corresponding to the same solar phase. It is clear that positive solar lags do not make any logical sense, because rainfall cannot influence solar activity. Therefore, the only real possibility for a positive link between solar activity and precipitation would be a lag of -105 months. This would mean that a solar maximum would trigger a precipitation maximum nearly 9 years later. It is unclear how such a long delay could be explained and transported in the climate system, even though it is not entirely impossible. We therefore favour the possibility that actually the solar minimum triggers the precipitation maximum in this region during February. The solar lags for the most negative r values is -50 to -35 months, meaning that the inverse rainfall effect would take place about 4-3 years after the solar trigger.

This would also explain why most studies from Western and Central Europe on various time scales have found generally higher rainfall and flood activity associated with low (rather than high) solar activity

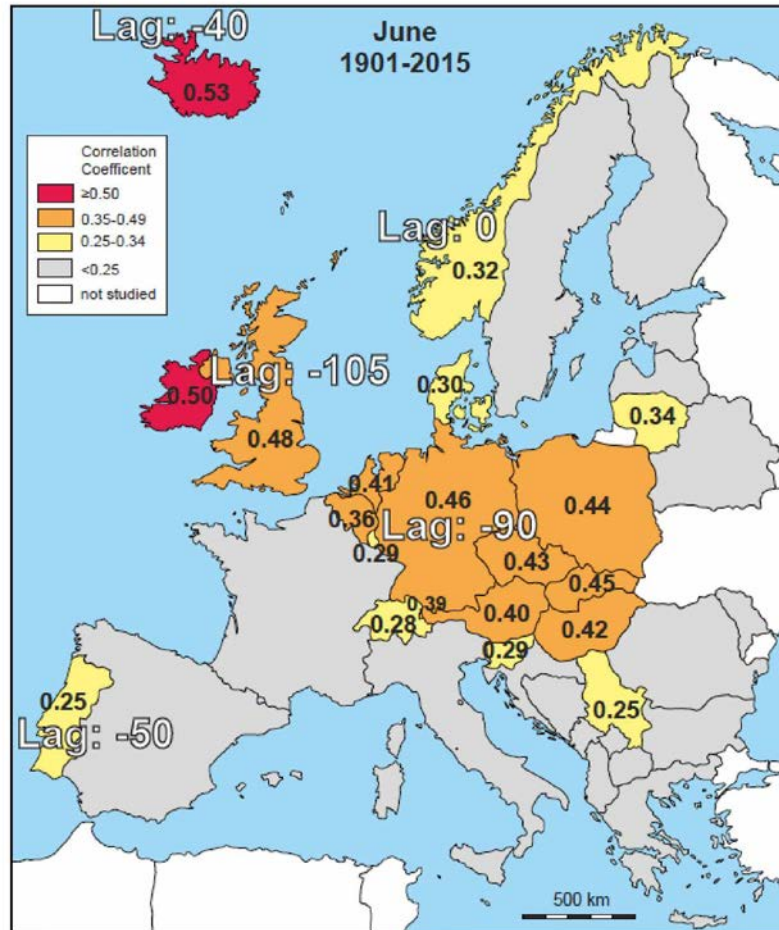


Fig. 6. Map showing the 1901–2015 most positive correlation coefficients for June precipitation and sunspots on a country-by-country basis. Pearson r values from Table 1, lags are from Table S1.

(e.g. Czymzik et al., 2016a; Mauquoy et al., 2004; Negendank et al., 1997; Swindles et al., 2012; Vos et al., 1997). Other authors have already noted such lead/lag relationships in which the solar trigger led hydroclimate by a few years (e.g. Czymzik et al., 2016b; Franke and Bechteler, 1969; Mares et al., 2016; Schwander et al., 2017). This may be particularly noteworthy for multidecadal flood maxima which may be best explained by the more abundant blocking events during phases of low solar activity (Czymzik et al., 2016a; Rimbu et al., 2017; Schwander et al., 2017). A similar time lag was described for the quasi-decadal NAO variability which is synchronized by the solar Schwabe cycle (Thieblemont et al., 2015). NAO+ (NAO-) typically lags the solar maximum (minimum) by a few years, possibly due to accumulation and memory effects in the Atlantic (Andrews et al., 2015; Gray et al., 2013, 2016; Ma et al., 2018; Roy et al., 2016; Scaife et al., 2013; Sfică et al., 2015; Sjolte et al., 2018; Thieblemont et al., 2015; Zhou et al., 2014). Processes in the atmosphere are too fast-paced and cannot provide significant time lags (Andrews et al., 2015). Regardless of the exact trigger mechanisms, visual inspection of the unshifted time series of sunspots and February precipitation in Germany and neighbouring countries suggests a generally positive relationship between the two

parameters (Figs. 1 and S1). This is because the zero time lag line in the r-against-lag diagram plots closer to the Pearson r maximum than to the minimum (Fig. 9). Empirically, this means more precipitation during times of higher solar activity, even though peak precipitation occurs 20 months

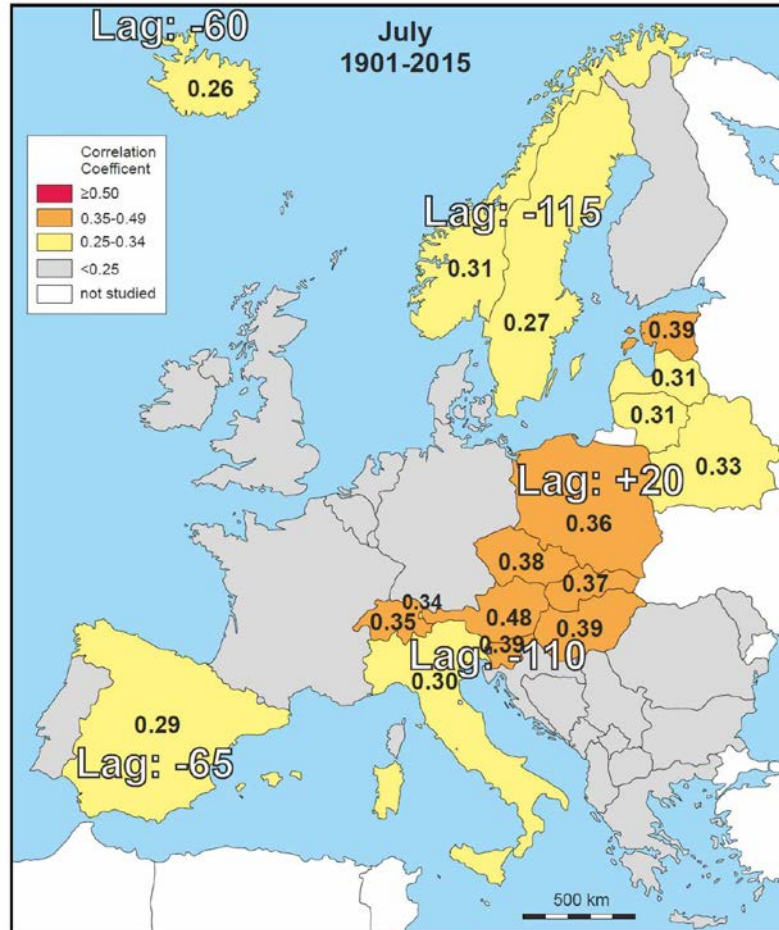


Fig. 7. Map showing the 1901–2015 most positive correlation coefficients for July precipitation and sunspots on a country-by-country basis. Pearson r values from Table 1, lags are from Table S1.

before the Schwabe maximum. The area of maximum solar influence on precipitation is located in central and western Europe which is significantly affected by the westerlies that typically transport rain to the region. During low solar activity winters, westerlies are reported to be weaker and occur less often in central Europe ([Ineson et al., 2011](#); [Schwander et al., 2017](#)), because intense and long lasting winter blocking events become more frequent, disrupting the westerly winds ([Barriopedro et al., 2008](#); [Lockwood et al., 2010](#)). The solar effect may fade out towards Eastern Europe because cold continental arctic conditions prevail here in winter (Fig. 3). During times of high solar activity, the westerlies are stronger, more persistent and less interrupted by blockings, bringing increased amounts of rain to central Europe. Long-term trends of solar activity and the North Atlantic Oscillation (NAO) were mostly in-phase since 1940, implying that low and high solar activity were typically associated with NAO- and NAO + conditions, respectively ([Gray et al., 2013](#); [Scaife et al., 2013](#); [Thieblemont et al., 2015](#)). During NAO- conditions, the westerly storm belt typically shifts southwards to southern Europe, leading to increased amounts of rain there, whilst resulting in reduced precipitation in central Europe ([Morley et al., 2014](#); [Wirth et al., 2013b](#)). Correspondingly,

the westerly storm belt hits central Europe during NAO + conditions, bringing increased amounts of rain there. The phase relationship between solar and precipitation maxima is not entirely stable. In the case of central Europe, the best correlations exist from the 1920s to the mid 2000s (Figs. 1 and 2). Phase shifts occur before and after this interval. This interval of best correlations corresponds

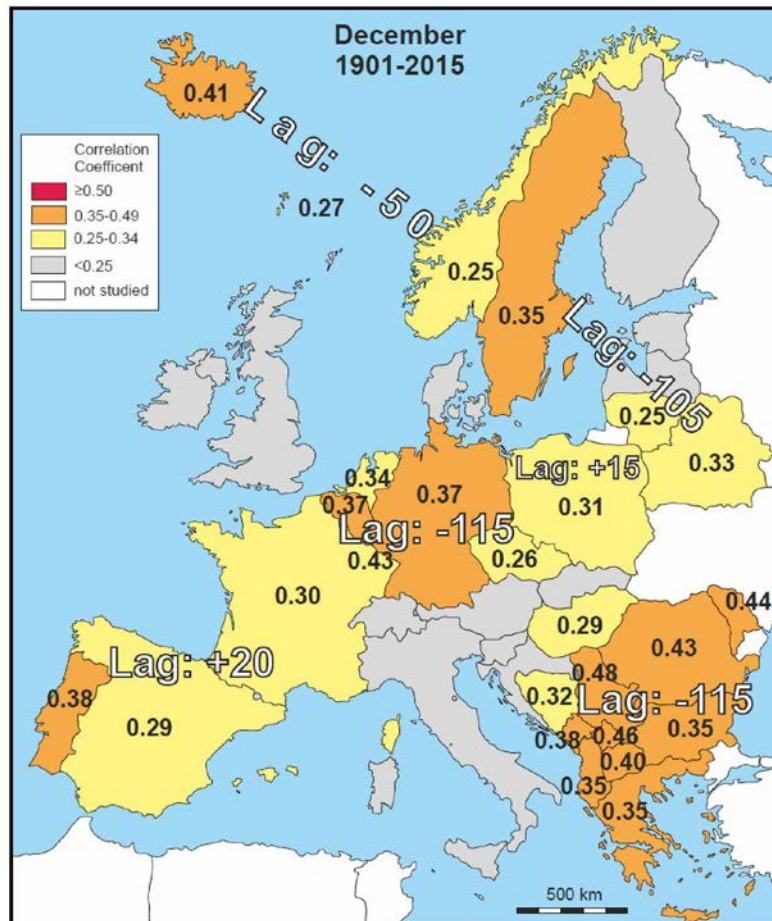


Fig. 8. Map showing the 1901–2015 most positive correlation coefficients for December precipitation and sunspots on a country-by-country basis. Pearson r values from Table 1, lags are from Table S1.

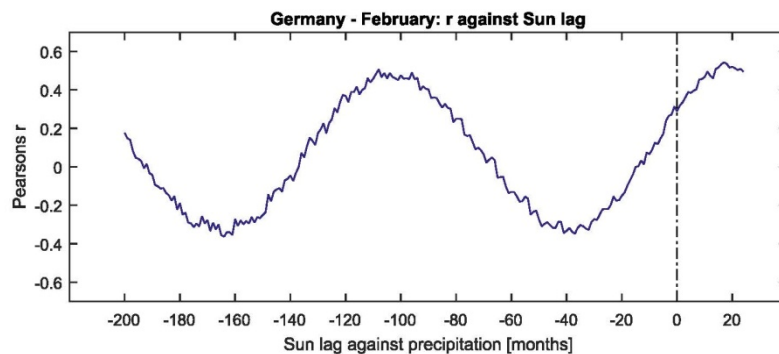


Fig. 9. Plot of Pearson r (precipitation vs. solar) against solar lag for February precipitation in Germany. Negative solar lags indicate that solar development leads the precipitation. Positive solar lags are just theoretical, because physically impossible.

generally to the maximum of the solar Gleissberg cycle (70–100 years) when multidecadal trends of NAO and solar activity run in parallel and are positively correlated (van Loon et al., 2012) (Fig. S22). During Gleissberg Minima, however, the two trends are opposite and are negatively correlated. The reasons for these phase reversals in correlation are still unclear and may be due to equator to pole temperature gradients (van Loon et al., 2012), or in the solar dynamo fields (Georgieva et al., 2012). The variable relationship between solar forcing and NAO has also been discussed by Sjolte et al. (2018). As the detailed processes involved in solar forcing of European hydroclimate are still poorly understood, the influence of the solar magnetic and geomagnetic fields has to be included in the lead/lag considerations. Notably, cosmic ray variations seen by neutron monitors lag sunspot number variations by up to 14 months in odd numbered cycles, whilst only by 2 months in even numbered cycles (Hathaway, 2015). The search for cause-effect is further complicated by the fact that some hydrological processes, e.g. European extreme precipitation, are influenced by the preceding wintertime NAO with time lags of one, two and three seasons (Tabari and Willems, 2018). This points to multiyear chains of coupled lags, linking the solar signal with ocean cycles and subsequently with the final hydroclimatic effect.

5.2. May

May rainfall responds very differently to the solar signal than in the preceding and subsequent months (February–July). The best Pearson r values are negative and occur in northeastern Europe (Czech Republic, Poland, Belarus) with a typical solar lag of +15 months (Fig. S13). High solar activity commonly results in low precipitation, a relationship that is well illustrated in the unshifted and shifted May time series of e.g. Belarus (Figs. 5 and S2). The exact meteorological reasons for this shortterm phase shift in May are unclear.

5.3. Summer months

June and July are typically the wettest months in Central Europe. As the summer develops, the area of solar influence on precipitation gradually migrates from the British Isles southeastwards via Germany into SE Central Europe (Figs. 6 and 7). High solar activity appears to push rain-bearing westerlies gradually deeper into Eastern Europe. By August, the solar-influenced rain belt reaches its most easterly position and is restricted to Belarus ($r=0.35$) and Moldova ($r=0.32$) (Table 1, Fig. S6). Drought conditions in June/July 2018 in Germany support the observed relationship. Rainfall reached only 50–60% of the long term normal, coinciding with a solar activity minimum regime of solar cycle 24. Likewise, June 2018 in England and Wales ranked within the top five driest Junes on record with figures dating back to 1910.

5.4. December

Increased solar activity appears to mildly stimulate precipitation in a southwest-northeast trending corridor reaching from Iberia to Belarus (Fig. 8). This effect could be related to rain-bearing southwesterly winds from the Atlantic, which may be stronger when the sun is more active. Notably for Iberia, the December effect at first sight appears to deviate from the general link of reduced solar activity, negative NAO and increased precipitation which dominates for most of the rest of the cold season in Iberia (Hurrell et al., 2003; Vicente-Serrano et al., 2011). Considering that the NAO lags the

solar Schwabe signal by up to half a solar cycle, the relationship may in fact be true here as well. The solar influence on the Balkan in December is still poorly understood and may be unrelated to the westerlies.

5.5. Mid-term forecasting potential

The near-cyclical nature of the ~ 11 years solar Schwabe cycle and the empirically identified lead/lag relationships with precipitation open up opportunities for improved mid-term prognoses that could be valuable for agricultural purposes, flood risk preparedness and other fields of human activity. An example is the anomalously low precipitation recorded in Germany during February 2018 (17.8 mm), representing only 36% of the long term average ([DWD, 2018](#)). The anomaly occurred exactly four years after an early 2014 activity spike in solar activity, associated with the maximum of the 24th solar cycle (Fig. S14). A closer look at the development 2000–2018 points to a possible pattern. For example, a similar solar activity spike during 2011 was followed by another very dry February in Germany (2015), again a delay of 4 years (Fig. S14). In contrast, the very wet year 2016 was preceded by relatively lower solar activity in 2012. The observations fit with the hypothesis of a negative correlation between solar activity and February rain in Central Europe, whereby the precipitation effect is delayed by up to 50 months (solar lag= -50). It may also be worth experimenting with rolling averages of solar activity rather than specific monthly values, in order to adjust for significant solar variability in certain years. Whilst February yields the best correlation coefficients in Europe, precipitation of other months also shows a clear link to solar variability, even though of weaker coupling. In Central Europe and parts of Scandinavia, the months of March, April, June and July show a correlation and phase pattern that has similarities with February. As these months comprise a significant part of the agricultural growing season, which in Germany lasts from March to October, any forecasting potential has economic significance. In Iberia, the months of February, April, August and December show noteworthy correlations that could be used to develop mid-term forecasts. On the Balkans, the months of February, April, November and December look most promising. The negative r coefficient of $r=-0.43$ for Greece with a negligible lag (Tables S2 and S3) suggests an inverse relationship between February rain and solar activity in that country. If the empirically identified relationship stays stable, February precipitation in Greece is expected to be reduced during 2019–2023 because of the expected development of the solar minimum associated with the transition between solar cycles 24 and 25. In this contribution we focus on the link between solar activity and precipitation. Nevertheless, other important mechanisms play a major role in controlling variability of European hydroclimate. Future research will have to fully integrate the solar results with the known influence of the NAO and the Atlantic Multidecadal Oscillation (AMO). Despite the temporal and spatial complexity, some systematic patterns begin to emerge that may help to eventually understand the meteorological mechanisms behind these hydroclimatic changes. Non-linear responses and phase shifts complicate the picture. Considering that large amounts of observational data are now available, it may be worth considering artificial intelligence and machine learning techniques (e.g. [Jones, 2017](#)) to get a full view of the dependencies and possible processes included in the variability of European precipitation.

6. Conclusions

European hydroclimate shows a high degree of variability on every time scale. The variability is controlled by natural processes such as Atlantic ocean cycles, changes in solar activity, volcanic activity and anthropogenic factors. This contribution concentrates on the solar influence on European precipitation, which has been documented by a large body of published case studies. We are concentrating on the period 1901–2015 for which we compare monthly precipitation series of 39 European countries with sunspot data by calculating Pearson correlation coefficients for a multi-year cross-correlation window. The results have been mapped out across the continent in order to identify areas in which solar activity may have influenced precipitation. February precipitation in Central and Western Europe shows the strongest solar response with coefficients reaching up to +0.61. Rainfall in June–July is also co-driven by solar activity changes, whereby the solar-influenced zone of rainfall gradually migrates from the British Isles southeastwards via Germany into SE Central Europe. On a decadal scale, the correlation between precipitation and solar activity in central Europe during these months appears to be positive, both statistically and by visual curve comparison. Yet, best positive correlations coefficients of February, June, July and December are typically reached when the solar signal lags rainfall by 1.5–2 years. Honouring cause and effect, it is suspected that increases in rainfall are actually triggered by the solar minimum some 3–4 years before the rainfall month. Lags of a few years also occur between solar activity and the solar-synchronized-NAO, possibly due to memory effects in the Atlantic. A lag in rainfall relative to the solar signal may open up new possibilities for forecasts, likely with enormous economic significance. The literature review demonstrates that most multidecadal studies from Central Europe encountered a negative correlation between solar activity and rainfall, probably because short time lags of a few years are negligible on timescales beyond the 11 year solar Schwabe cycle. Flood frequency typically increases during times of low solar activity associated with negative NAO conditions and more frequent blocking. The Alps form the southern limit of the Central European solar-driven rainfall region because solar/rain relationships in the southern Alps appear to flip ([Pena et al., 2015](#); [Rabadan and Schulte, 2014](#)). Future research on the solar influence on European rainfall may also have to consider possible effects of the 22 year solar Hale cycle, which represents a full magnetic cycle after two Schwabe magnetic polarity reversals ([Dobrica et al., 2017](#); [Zanchettin et al., 2008](#)).

Acknowledgements

We thank Josef Kowatsch, Steven Michelbach and Frank Bosse for valuable discussions. We are grateful to Denis Fourgassie (Meteo-France), Mark Beswick (Met Office National Meteorological Archive) and Hans Bengtsson (Swedish Meteorological and Hydrological Institute, SMHI) for providing long historical rainfall series for Paris, Edinburgh and Stockholm. The vectorised Europe base map in this paper was sourced from www.d-maps.com, a useful service for which we are thankful. We are extremely grateful to the anonymous reviewers whose valuable comments stimulated us to expand our study and include some important additional aspects.

Appendix A. Supplementary data

Supplementary data to this article can be found online at <https://doi.org/10.1016/j.jastp.2019.01.012>.

References

- [Andrews, M.B., Knight, J.R., Gray, L.J., 2015. A simulated lagged response of the North Atlantic Oscillation to the solar cycle over the period 1960–2009. *Environ. Res. Lett.* 10 \(5\), 054022.](#)
- [Barrera-Escoda, A., Llasat, M.C., 2015. Evolving flood patterns in a Mediterranean region \(1301–2012\) and climatic factors – the case of Catalonia. *Hydrol. Earth Syst. Sci.* 19 \(1\), 465–483.](#)
- [Barriopedro, D., Garcia-Herrera, R., Huth, R., 2008. Solar modulation of Northern Hemisphere winter blocking. *J. Geophys. Res.: Atmosphere* 113, D14.](#)
- [Blaauw, M., van Geel, B., van der Plicht, J., 2004. Solar forcing of climatic change during the mid-Holocene: indications from raised bogs in The Netherlands. *Holocene* 14 \(1\), 35–44.](#)
- [Blackford, J.J., Chambers, F.M., 1995. Proxy climate record for the last 1000 years from Irish blanket peat and a possible link to solar variability. *Earth Planet. Sci. Lett.* 133 \(1\), 145–150.](#)
- [Bond, G., Kromer, B., Beer, J., Muscheler, R., Evans, M.N., Showers, W., Hoffmann, S., Lotti-Bond, R., Hajdas, I., Bonani, G., 2001. Persistent solar influence on North Atlantic climate during the Holocene. *Science* 294, 2130–2136.](#)
- [Bothe, O., Wagner, S., Zorita, E., 2018. Inconsistencies between observed, reconstructed, and simulated precipitation over the British Isles during the last 350 years. *Clim. Past Discuss* 1–28 2018.](#)
- [Brunetti, M., Maugeri, M., Nanni, T., 2000. Variations of temperature and precipitation in Italy from 1866 to 1995. *Theor. Appl. Climatol.* 65 \(3\), 165–174.](#)
- [Camuffo, D., Enzi, S., 1995. Climatic features during the Sporer and Maunda minima. In: Frenzel, B. \(Ed.\), *Solar Output and Climate during the Holocene, Paleoclimate Research, Special Issue 16*. Fischer Verlag, Stuttgart, pp. 105–125.](#)
- [Chen, L., Zonneveld, K.A.F., Versteegh, G.J.M., 2011. Short term climate variability during “Roman classical period” in the eastern mediterranean. *Quat. Sci. Rev.* 30 \(27–28\), 3880–3891.](#)
- [Cini Castagnoli, G., Bonino, G., Taricco, C., Bernasconi, S.M., 2002. Solar radiation variability in the last 1400 years recorded in the carbon isotope ratio of a mediterranean sea core. *Adv. Space Res.* 29 \(12\), 1989–1994.](#)
- [Clette, F., Svalgaard, L., Vaquero, J.M., Cliver, E.W., 2015. Revisiting the sunspot number. In: Balogh, A., Hudson, H., Petrovay, K., von Steiger, R. \(Eds.\), *The Solar Activity Cycle: Physical Causes and Consequences*. Springer, New York, NY, pp. 35–103 New York.](#)
- [Corella, J.P., Benito, G., Rodriguez-Lloveras, X., Brauer, A., Valero-Garces, B.L., 2014. Annually-resolved lake record of extreme hydro-meteorological events since AD 1347 in NE Iberian Peninsula. *Quat. Sci. Rev.* 93, 77–90.](#)
- [Czymzik, M., Brauer, A., Dulski, P., Plessen, B., Naumann, R., von Grafenstein, U., Scheffler, R., 2013. Orbital and solar forcing of shifts in Mid- to Late Holocene flood intensity from varved sediments of pre-alpine Lake Ammersee \(southern Germany\). *Quat. Sci. Rev.* 61, 96–110.](#)
- [Czymzik, M., Dreibrodt, S., Feeser, I., Adolphi, F., Brauer, A., 2016a. Mid-Holocene humid periods reconstructed from calcite varves of the Lake Woserin sediment record \(north-eastern Germany\). *Holocene* 26 \(6\), 935–946.](#)
- [Czymzik, M., Dulski, P., Plessen, B., von Grafenstein, U., Naumann, R., Brauer, A., 2010. A 450 year record of spring-summer flood layers in annually laminated sediments from Lake Ammersee \(southern Germany\). *Water Resour. Res.* 46 \(11\).](#)
- [Czymzik, M., Muscheler, R., Brauer, A., 2016b. Solar modulation of flood frequency in central Europe during spring and summer on interannual to multi-centennial timescales. *Clim. Past* 12 \(3\), 799–805.](#)
- [DeAngelis, A.M., Qu, X., Zelinka, M.D., Hall, A., 2015. An observational radiative constraint on hydrologic cycle intensification. *Nature* 528, 249.](#)
- [Dobrica, V., Demetrescu, C., Mares, I., Mares, C., 2017. Long-term Evolution of the Lower Danube Discharge and Corresponding Climate Variations: Solar Signature Imprint: Theoretical and Applied Climatology.](#)
- [Ducic, V., Lukovic, J., Nikolova, N., 2007. Possible connection between Danube river discharge variability and solar activity. *Bull. Serbian Geograph. Soc.* 1, 31–38.](#)
- [DWD, 2018. The weather in Germany in February 2018. \[https://www.dwd.de/DE/presse/pressemitteilungen/DE/2018/20180227_deutschlandwetter_februar_news.html\]\(https://www.dwd.de/DE/presse/pressemitteilungen/DE/2018/20180227_deutschlandwetter_februar_news.html\).](#)

- [Franke, P.G., Bechteler, W., 1969. Relation between Sunspots and Discharge: the Use of Analog and Digital Computers in Hydrology: Proceedings of the Tucson Symposium. pp. 527–530.](#)
- [Georgieva, K., Kirov, B., Koucka Knižova, P., Mošna, Z., Kouba, D., Asenovska, Y., 2012. Solar influences on atmospheric circulation. *J. Atmos. Sol. Terr. Phys.* 90–91, 15–25.](#)
- [Glaser, R., Riemann, D., Schonbein, J., Barriendos, M., Brazdil, R., Bertolin, C., Camuffo, D., Deutsch, M., Dobrovolny, P., van Engelen, A., Enzi, S., Haličková, M., Koenig, S.J., Kotyza, O., Limanowka, D., Mackova, J., Sghedoni, M., Martin, B., Himmelsbach, I., 2010. The variability of European floods since AD 1500. *Climatic Change* 101 \(1\), 235–256.](#)
- [Gray, L.J., Scaife, A.A., Mitchell, D.M., Osprey, S., Ineson, S., Hardiman, S., Butchart, N., Knight, J., Sutton, R., Kodera, K., 2013. A lagged response to the 11 year solar cycle in observed winter Atlantic/European weather patterns. 13. *J. Geophys. Res.: Atmosphere* 118 \(24\), 405–413 420.](#)
- [Gray, L.J., Woollings, T.J., Andrews, M., Knight, J., 2016. Eleven-year solar cycle signal in the NAO and Atlantic/European blocking. *Q. J. R. Meteorol. Soc.* 142 \(698\), 1890–1903.](#)
- [Grinsted, A., Moore, J.C., Jevrejeva, S., 2004. Application of the cross wavelet transform and wavelet coherence to geophysical time series. *Nonlinear Process Geophys.* 11 \(5/6\), 561–566.](#)
- [Hajian, S., Movahed, M.S., 2010. Multifractal Detrended Cross-Correlation Analysis of sunspot numbers and river flow fluctuations. *Phys. Stat. Mech. Appl.* 389 \(21\), 4942–4957.](#)
- [Hathaway, D.H., 2015. The solar cycle. *Living Rev. Sol. Phys.* 12 \(1\), 4.](#)
- [Hoerling, M., Eischeid, J., Perlwitz, J., 2009. Regional precipitation trends: distinguishing natural variability from anthropogenic forcing. *J. Clim.* 23 \(8\), 2131–2145.](#)
- [Hurrell, J.W., Kushnir, Y., Ottersen, G., Visbek, M., 2003. An overview of the north Atlantic oscillation. In: In: Hurrell, J.W., Kushnir, Y., Ottersen, G., Visbeck, M. \(Eds.\), *The North Atlantic Oscillation: Climatic Significance and Environmental Impact*, vol 134. American Geophysical Union, Geophysical Monograph Series, pp. 1–35.](#)
- [Hurrell, J.W., van Loon, H., 1997. Decadal variations in climate associated with the north Atlantic oscillation. *Climatic Change* 36 \(3\), 301–326.](#)
- [Ineson, S., Scaife, A.A., Knight, J.R., Manners, J.C., Dunstone, N.J., Gray, L.J., Haigh, J.D., 2011. Solar forcing of winter climate variability in the Northern Hemisphere. *Nat. Geosci.* 4, 753–757.](#)
- [Jones, N., 2017. How machine learning could help to improve climate forecasts. *Nature* 548, 379–380.](#)
- [Kantelhardt, J.W., 2004. Fluktuationen in Komplexen Systemen. Habilitation Thesis. Justus-Liebig-University Giesen, pp. 217. <http://www.physik.uni-halle.de/Fachgruppen/kantel/habil.pdf>.](#)
- [Kantelhardt, J.W., Koscielny-Bunde, E., Rego, H.H.A., Havlin, S., Bunde, A., 2001. Detecting long-range correlations with detrended fluctuation analysis. *Phys. Stat. Mech. Appl.* 295 \(3\), 441–454.](#)
- [Kilian, M.R., Van der Plicht, J., Van Geel, B., 1995. Dating raised bogs: new aspects of AMS 14C wiggle matching, a reservoir effect and climatic change. *Quat. Sci. Rev.* 14 \(10\), 959–966.](#)
- [Kokfelt, U., Muscheler, R., 2013. Solar forcing of climate during the last millennium recorded in lake sediments from northern Sweden. *Holocene* 23 \(3\).](#)
- [Labuhn, I., Hammarlund, D., Chapron, E., Czymzik, M., Dumoulin, J.-P., Nilsson, A., Regnier, E., Robygd, J., von Grafenstein, U., 2018. Holocene hydroclimate variability in central Scandinavia inferred from flood layers in contourite drift deposits in lake Storsjon. *Quaternary* 1 \(1\), 2.](#)
- [Lamy, F., Arz, H.W., Bond, G.C., Bahr, A., Patzold, J., 2006. Multicentennial-scale hydrological changes in the Black Sea and northern red sea during the Holocene and the arctic/North Atlantic oscillation. *Paleoceanography* 21 \(1\) n/a-n/a.](#)
- [Landscheidt, T., 2000. River Po discharges and cycles of solar activity. *Hydrol. Sci. J.* 45 \(3\), 491–493.](#)
- [Le Mouel, J.-L., Blanter, E., Shnirman, M., Courtillot, V., 2009. Evidence for solar forcing in variability of temperatures and pressures in Europe. *J. Atmos. Sol. Terr. Phys.* 71 \(12\), 1309–1321.](#)
- [Linderholm, H.W., Nicolle, M., Francus, P., Gajewski, K., Helama, S., Korhola, A., Solomina, O., Yu, Z., Zhang, P., D'Andrea, W.J., Debret, M., Divine, D.V., Gunnarson, B.E., Loader, N.J., Massei, N., Seftigen, K., Thomas, E.K., Werner, J., Andersson, S.,](#)

- [Bertsson, A., Luoto, T.P., Nevalainen, L., Saarni, S., Valiranta, M., 2018. Arctic hydroclimate variability during the last 2000 years: current understanding and research challenges. *Clim. Past* 14 \(4\), 473–514.](#)
- [Lockwood, M., Harrison, R.G., Woollings, T., Solanki, S.K., 2010. Are cold winters in Europe associated with low solar activity? *Environ. Res. Lett.* 5, 1–7.](#)
- [Luo, J., Ying, K., He, P., Bai, J., 2005. Properties of Savitzky–golay digital differentiators. *Digit. Signal Process.* 15 \(2\), 122–136.](#)
- [Ma, H., Chen, H., Gray, L., Zhou, L., Li, X., Wang, R., Zhu, S., 2018. Changing response of the North Atlantic/European winter climate to the 11 year solar cycle. *Environ. Res. Lett.* 13 \(3\), 034007.](#)
- [Macklin, M.G., Johnstone, E., Lewin, J., 2005. Pervasive and long-term forcing of Holocene river instability and flooding in Great Britain by centennial-scale climate change. *Holocene* 15 \(7\), 937–943.](#)
- [Magny, M., 1993. Solar influences on Holocene climatic changes illustrated by correlations between past lake-level fluctuations and the atmospheric 14C record. *Quat. Res.* 40, 1–9.](#)
- [Magny, M., 2004. Holocene climate variability as reflected by mid-European lake-level fluctuations and its probable impact on prehistoric human settlements. *Quat. Int.* 113, 65–79.](#)
- [Maraun, D., 2013. When will trends in European mean and heavy daily precipitation emerge? *Environ. Res. Lett.* 8 \(1\), 014004.](#)
- [Mares, I., Dobrica, V., Demetrescu, C., Mares, C., 2016. Hydrological response in the Danube lower basin to some internal and external climate forcing factors: *Hydrol. Earth Syst. Sci. Data* 1–24 2016.](#)
- [Markonis, Y., Hanel, M., Maca, P., Kysely, J., Cook, E.R., 2018. Persistent multi-scale fluctuations shift European hydroclimate to its millennial boundaries. *Nat. Commun.* 9 \(1\), 1767.](#)
- [Martin-Puertas, C., Matthes, K., Brauer, A., Muscheler, R., Hansen, F., Petrick, C., Aldahan, A., Possnert, G., Geel, B. v., 2012. Regional atmospheric circulation shifts induced by a grand solar minimum. *Nat. Geosci.* <https://doi.org/10.1038/ngeo1460>.](#)
- [Mauquoy, D., Engelkes, T., Groot, M.H.M., Markesteijn, F., Oudejans, M.G., van der Plicht, J., van Geel, B., 2002. High-resolution records of late-Holocene climate change and carbon accumulation in two north-west European ombrotrophic peat bogs. *Palaeogeogr. Palaeoclimatol. Palaeoecol.* 186 \(3\), 275–310.](#)
- [Mauquoy, D., van Geel, B., Blaauw, M., Speranza, A., van der Plicht, J., 2004. Changes in solar activity and Holocene climatic shifts derived from 14C wiggle-match dated peat deposits. *Holocene* 14 \(1\), 45–52.](#)
- [Mauquoy, D., Yeloff, D., Van Geel, B., Charman, D.J., Blundell, A., 2008. Two decadal resolved records from north-west European peat bogs show rapid climate changes associated with solar variability during the mid–late Holocene. *J. Quat. Sci.* 23 \(8\), 745–763.](#)
- [Mazhdraikov, M., Benov, D., Valkanov, N., 2018. *The Monte Carlo Method: Engineering Applications*. ACMO Academic Press, Sofia, pp. 235.](#)
- [Mellstrom, A., van der Putten, N., Muscheler, R., de Jong, R., Bjorck, S., 2015. A shift towards wetter and windier conditions in southern Sweden around the prominent solar minimum 2750 cal a BP. *J. Quat. Sci.* 30 \(3\), 235–244.](#)
- [Moreno, A., Valero-Garces, B.L., Gonzalez-Samperiz, P., Rico, M., 2008. Flood response to rainfall variability during the last 2000 years inferred from the Taravilla Lake record \(Central Iberian Range, Spain\). *J. Paleolimnol.* 40 \(3\), 943–961.](#)
- [Morley, A., Rosenthal, Y., deMenocal, P., 2014. Ocean-atmosphere climate shift during the mid-to-late Holocene transition. *Earth Planet. Sci. Lett.* 388, 18–26.](#)
- [Negendank, J.F.W., Zolitschka, B., Rein, B., Brauer, A., Bruchmann, C., Sanchez, A., Vos, H., 1997. Varve chronology and solar variability in lake Holzmaar \(Eifel, Germany\), *Bulletin de la Societe belge de Geologie* 106, 53–61.](#)
- [Nurtaev, B., 2015. Influence of climate variability on large rivers runoff. *Proc. IAHS* 371, 211–214.](#)
- [Peña, J.C., Schulte, L., Badoux, A., Barriendos, M., Barrera-Escoda, A., 2015. Influence of solar forcing, climate variability and modes of low-frequency atmospheric variability on summer floods in Switzerland: *Hydrol. Earth Syst. Sci.* 19 \(9\), 3807–3827.](#)
- [Rabadan, J.C.P., Schulte, L., 2014. Effects of solar activity and climate variability on large floods in Switzerland. *Boletín de la Asociación de Geógrafos Españoles* 65, 469–475.](#)

- [Rao, M.P., Cook, B.I., Cook, E.R., D'Arrigo, R.D., Krusic, P.J., Anchukaitis, K.J., LeGrande, A.N., Buckley, B.M., Davi, N.K., Leland, C., Griffin, K.L., 2017. European and Mediterranean hydroclimate responses to tropical volcanic forcing over the last millennium. *Geophys. Res. Lett.* 44 \(10\), 5104–5112.](#)
- [Riley, K.F., Hobson, M.P., Bence, S.J., 2006. *Mathematical Methods for Physics and Engineering: A Comprehensive Guide*. Cambridge University Press, Cambridge.](#)
- [Rimbu, N., Ionita, M., Czymzik, M., Brauer, A., Lohmann, G., 2017. Patterns of extreme weather associated with observed and proxy River Ammer flood records. *Clim. Past Discuss* 1–27 2017.](#)
- [Roy, I., Asikainen, T., Maliniemi, V., Mursula, K., 2016. Comparing the influence of sunspot activity and geomagnetic activity on winter surface climate. *J. Atmos. Sol. Terr. Phys.* 149, 167–179.](#)
- [Savitzky, A., Golay, M.J.E., 1964. Smoothing and differentiation of data by simplified least squares procedures. *Anal. Chem.* 36 \(8\), 1627–1639.](#)
- [Scaife, A.A., Ineson, S., Knight, J.R., Gray, L., Kodera, K., Smith, D.M., 2013. A mechanism for lagged North Atlantic climate response to solar variability. *Geophys. Res. Lett.* 40 \(2\), 434–439.](#)
- [Schulte, L., Pena, J.C., Carvalho, F., Schmidt, T., Julia, R., Llorca, J., Veit, H., 2015. A 2600-year history of floods in the Bernese Alps, Switzerland: frequencies, mechanisms and climate forcing: *Hydrol. Earth Syst. Sci.* 19 \(7\), 3047–3072.](#)
- [Schulte, L., Veit, H., Burjachs, F., Julia, R., 2009. Lutschine fan delta response to climate variability and land use in the Bernese Alps during the last 2400 years. *Geomorphology* 108 \(1\), 107–121.](#)
- [Schwander, M., Rohrer, M., Bronnimann, S., Malik, A., 2017. Influence of solar variability on the occurrence of central European weather types from 1763 to 2009. *Clim. Past* 13 \(9\), 1199–1212.](#)
- [Sfică, L., Voiculescu, M., Huth, R., 2015. The influence of solar activity on action centres of atmospheric circulation in North Atlantic. *Ann. Geophys.* 33 \(2\), 207–215.](#)
- [Sjolte, J., Sturm, C., Adolphi, F., Vinther, B.M., Werner, M., Lohmann, G., Muscheler, R., 2018. Solar and volcanic forcing of North Atlantic climate inferred from a processbased reconstruction. *Clim. Past Discuss* 1–22 2018.](#)
- [Smith, A.C., Wynn, P.M., Barker, P.A., Leng, M.J., Noble, S.R., Tych, W., 2016. North Atlantic forcing of moisture delivery to Europe throughout the Holocene. *Sci. Rep.* 6, 24745.](#)
- [Speranza, A., van Geel, B., van der Plicht, J., 2003. Evidence for solar forcing of climate change at ca. 850 cal BC from a Czech peat sequence. *Glob. Planet. Chang.* 35 \(1\), 51–65.](#)
- [Stolze, S., Muscheler, R., Dorfler, W., Nelle, O., 2013. Solar influence on climate variability and human development during the Neolithic: evidence from a high-resolution multi-proxy record from Templevanny Lough, County Sligo, Ireland. *Quat. Sci. Rev.* 67, 138–159.](#)
- [Sun, Q., Miao, C., Duan, Q., Ashouri, H., Sorooshian, S., Hsu, K.-L., 2018. A review of global precipitation data sets: data sources, estimation, and intercomparisons. *Rev. Geophys.* 56 \(1\), 79–107.](#)
- [Swindles, G.T., Blundell, A., Roe, H.M., Hall, V.A., 2010. A 4500-year proxy climate record from peatlands in the North of Ireland: the identification of widespread summer 'drought phases'? *Quat. Sci. Rev.* 29 \(13\), 1577–1589.](#)
- [Swindles, G.T., Patterson, R.T., Roe, H.M., Galloway, J.M., 2012. Evaluating periodicities in peat-based climate proxy records. *Quat. Sci. Rev.* 41 \(0\), 94–103.](#)
- [Swindles, G.T., Plunkett, G., Roe, H.M., 2007a. A delayed climatic response to solar forcing at 2800 cal. BP: multiproxy evidence from three Irish peatlands. *Holocene* 17 \(2\), 177–182.](#)
- [Swindles, G.T., Plunkett, G., Roe, H.M., 2007b. A multiproxy climate record from a raised bog in County Fermanagh, Northern Ireland: a critical examination of the link between bog surface wetness and solar variability. *J. Quat. Sci.* 22 \(7\), 667–679.](#)
- [Tabari, H., Willems, P., 2018. Lagged influence of Atlantic and Pacific climate patterns on European extreme precipitation. *Sci. Rep.* 8 \(1\), 5748.](#)
- [Thieblemont, R., Matthes, K., Omrani, N.-E., Kodera, K., Hansen, F., 2015. Solar forcing synchronizes decadal North Atlantic climate variability. *Nat. Commun.* 6, 8268.](#)

[Tomasino, M., Valle, F.D., 2000. Natural climatic changes and solar cycles: an analysis of hydrological time series. *Hydrol. Sci. J.* 45 \(3\), 477–489.](#)

[Tomasino, M., Zanchettin, D., Traverso, P., 2004. Long-range forecasts of River Po discharges based on predictable solar activity and a fuzzy neural network model/Previsions a long terme des debits du Fleuve Po basees sur l'activite solaire previsible et sur un modele de reseau de neurones flou. *Hydrol. Sci. J.* 49 \(4\), null–684.](#)

[Trigo, R.M., Pozo-Vazquez, D., Osborn, T.J., Castro-Diez, Y., Gamiz-Fortis, S., Esteban-Parra, M.J., 2004. North Atlantic oscillation influence on precipitation, river flow and water resources in the Iberian Peninsula. *Int. J. Climatol.* 24 \(8\), 925–944.](#)

[Turcotte, D.L., 1997. *Fractals and Chaos in Geology and Geophysics*. Cambridge University Press, Cambridge.](#)

[Van Geel, B., Heijnis, H., Charman, D.J., Thompson, G., Engels, S., 2014. Bog burst in the eastern Netherlands triggered by the 2.8 kyr BP climate event. *Holocene* 24 \(11\), 1465–1477.](#)

[van Geel, B., Mauquoy, D., 2010. Peatland Records of Solar Activity: *PAGES News*, vol. 18. pp. 11–12.](#)

[Van Geel, B., Van Der Plicht, J., Kilian, M.R., Klaver, E.R., Kouwenberg, J.H.M., Renssen, H., Reynaud-Farrera, I., Waterbolk, H.T., 1997. The sharp rise of \$\Delta^{14}C\$ ca. 800 cal BC: possible causes, related climatic teleconnections and the impact on human environments. *Radiocarbon* 40 \(1\), 535–550.](#)

[Van Loon, H., Brown, J., Milliff, R.F., 2012. Trends in sunspots and North Atlantic sea level pressure. *J. Geophys. Res.* 117 \(D7\), D07106.](#)

[Vanniere, B., Magny, M., Joannin, S., Simonneau, A., Wirth, S.B., Hamann, Y., Chapron, E., Gilli, A., Desmet, M., Anselmetti, F.S., 2013. Orbital changes, variation in solar activity and increased anthropogenic activities: controls on the Holocene flood frequency in the Lake Ledro area. Northern Italy: *Clim. Past* 9 \(3\), 1193–1209.](#)

[Vaquero, J.M., 2004. Solar signal in the number of floods recorded for the tagus river basin over the last millennium. *Climatic Change* 66 \(1\), 23–26.](#)

[Vicente-Serrano, S.M., Trigo, R.M., Lopez-Moreno, J.I., Liberato, M.L.R., Lorenzo-Lacruz, J., Begueria, S., Moran-Tejeda, E., El Kenawy, A., 2011. Extreme winter precipitation in the Iberian Peninsula in 2010: anomalies, driving mechanisms and future projections. *Clim. Res.* 46 \(1\), 51–65.](#)

[Vines, R.G., 1985. European rainfall patterns. *J. Climatol.* 5 \(6\), 607–616.](#)

[Vos, H., Bruchmann, C., Lucke, A., Negendank, J.F.W., Schleser, G.H., Zolitschka, B., 2004. Phase stability of the solar Schwabe cycle in lake Holzmaar, Germany, and GISP2, Greenland, between 10,000 and 9,000 cal. BP. In: Fischer, H., Kumke, T., Lohmann, G., Floser, G., Miller, H., von Storch, H., Negendank, J.F.W. \(Eds.\), *The Climate in Historical Times: towards a Synthesis of Holocene Proxy Data and Climate Models*. Springer Berlin Heidelberg, Berlin, Heidelberg, pp. 293–317.](#)

[Vos, H., Sanchez, A., Zolitschka, B., Brauer, A., Negendank, J.F.W., 1997. Solar activity variations recorded in varved sediments from the Crater Lake of Holzmaar - a Maar Lake in the Westeifel volcanic field, Germany. *Surv. Geophys.* 18 \(2\), 163–182.](#)

[Wirth, S.B., Gilli, A., Simonneau, A., Ariztegui, D., Vanniere, B., Glur, L., Chapron, E., Magny, M., Anselmetti, F.S., 2013a. A 2000 year long seasonal record of floods in the southern European Alps. *Geophys. Res. Lett.* 40 \(15\), 4025–4029.](#)

[Wirth, S.B., Glur, L., Gilli, A., Anselmetti, F.S., 2013b. Holocene flood frequency across the Central Alps – solar forcing and evidence for variations in North Atlantic atmospheric circulation. *Quat. Sci. Rev.* 80, 112–128.](#)

[Zanchettin, D., Rubino, A., Traverso, P., Tomasino, M., 2008. Impact of variations in solar activity on hydrological decadal patterns in northern Italy. *J. Geophys. Res.* 113, D12102.](#)

[Zhou, L., Tinsley, B., Huang, J., 2014. Effects on winter circulation of short and long term solar wind changes. *Adv. Space Res.* 54 \(12\), 2478–2490.](#)

[Zvervaev, I.I., Allan, R.P., 2010. Summertime precipitation variability over Europe and its links to atmospheric dynamics and evaporation. *J. Geophys. Res.: Atmosphere* 115, D12.](#)